AJNR Am J Neuroradiol 26:1512–1520, June/July 2005

Dilatation of the Virchow-Robin Space Is a Sensitive Indicator of Cerebral Microvascular Disease: Study in Elderly Patients with Dementia

Tufail F. Patankar, Dipayan Mitra, Anoop Varma, Julie Snowden, David Neary, and Alan Jackson

BACKGROUND AND PURPOSE: **Virchow-Robin spaces (VRSs) are CSF spaces that accompany blood vessels as they perforate the brain substance. Dilatation of VRS is associated with microangiopathy. Microvascular disease has a major etiologic and pathogenetic role in dementias. To our knowledge, no investigators have looked at the relationship between dilated VRS on MR imaging and cerebral microvascular disease. The aim of our study was to test the hypothesis that dilatation of VRS is associated with subcortical vascular dementia.**

METHODS: **We recruited 75 patients with Alzheimer's disease ($n = 35$), ischemic vascular dementia ($n = 24$), or frontotemporal dementia ($n = 16$) and 35 healthy volunteers. We assessed deep white matter and periventricular hyperintensities and the severity of VRS dilatation, as scored on MR images. Statistical group comparisons and multiple regression analyses were performed to quantify the relationship between imaging features and diagnoses.**

RESULTS: **White matter lesions were more common in patients with ischemic vascular dementia than in those with Alzheimer's disease or healthy volunteers ($P < .01$). VRS scores were significantly higher in patients with vascular dementia than in patients with AD ($P < .001$), patients with FTD ($P < .01$), or healthy volunteers ($P < .001$). VRS scores accounted for 29% of the variance in the regression model, and scores for periventricular hyperintensity accounted for 2%.**

CONCLUSION: **VRS dilatation is common in diseases associated with microvascular abnormality and can be used as a diagnostic tool to differentiate vascular dementias from degenerative dementias.**

Virchow-Robin spaces (VRSs) are perivascular spaces that surround the perforating arteries that enter the brain. The spaces are normally microscopic, but when dilated, they may be seen on MR images. Even in the normal brain, some VRSs are usually seen in the area of the substantia innominata at the level of the anterior commissure, and a small number of dilated spaces may also be seen in the basal ganglia (BG) in up to 60% of individuals (1). VRSs can be identified by a combination of their typical location and their signal intensity characteristics. They are classically described as isointense to CSF on images obtained with all pulse sequences (1–4), and they are round or linear depending on the imaging plane (5), although their characteristics may vary from this pattern for a number of reasons. First, the small size of the VRS makes partial-volume effects common; therefore, measured signal intensities seldom equal those seen in pure CSF, although the changes in signal intensity between sequences are closely correlated (6). In addition, T1-weighted images with substantial flow sensitivity may show high signal intensity due to inflow effects (1). Even if we allow for these effects, the measured signal intensity in the VRS often slightly differs from that of true CSF. This finding has been attributed to the fact that VRS around intracerebral arteries may represent interstitial fluid trapped in the subpial or interpial space (6).

Many pathologic states result in abnormal dilatation of VRS, with increased numbers of spaces visible on MR imaging. These are seen particularly along the

Received August 12, 2004; accepted after revision December 3.

From the Institutions Imaging Science and Biomedical Engineering, School of Medicine, University of Manchester (T.F.P., D.M., A.J.), and the Cerebral Function Unit, Greater Manchester Neuroscience Centre, Hope Hospital, Salford (A.V., J.S., D.N.), UK.

Presented at the 42nd Annual Meeting of the American Society of Neuroradiology, Seattle, WA, June 5–11, 2004.

Address reprint requests to Dr Tufail Patankar Imaging Science and Biomedical Engineering, Department of Medicine, Stopford Building, University of Manchester, Oxford Road, M13 9PT, UK.

course of the penetrating striothalamic arteries in the BG, the external and extreme capsule and also along the course of penetrating arteries in the centrum semiovale and the ventral mesencephalic tegmentum (4, 7–21).

Pathologic dilatation of VRS is most commonly associated with arteriolar abnormalities that arise due to aging, diabetes, hypercholesterolemia, smoking, and hypertension and other vascular risk factors. This dilatation forms part of a histologic spectrum of abnormalities, which include old, small infarcts (type 1 changes); scars from small hematomas (type 2 changes); and dilatations of VRS (type 3 changes) (22). The presence of these abnormalities on histologic examination is believed to result from moderate-to-severe microangiopathy characterized by sclerosis, hyalinosis, and lipid deposits in the walls of small perforating arteries 50–400 ìm in diameter (22, 23). As the severity of the microangiopathy increases, microvessels demonstrate increasingly severe changes, with arterial narrowing, microaneurysms and pseudoaneurysms, onion skinning, mural calcification, and thrombotic and fibrotic luminal occlusions (22–24) Although microvascular disease is common, few reliable surrogate imaging markers of its presence have been described. The extent and severity of deep white matter (WM) and periventricular hyperintensity on T2-weighted images have been widely studied as potential surrogate markers for small-vessel disease. However, the correlation between these abnormalities and clinical characteristics, such as diagnosis, vascular risk factor, or neuropsychological deficit, is often poor (25–32).

Therefore, the purpose of this study was to test the hypothesis that abnormal dilatation of VRS is a potential surrogate marker of microvascular disease in patients with dementing illness.

Methods

Subjects were recruited from four health districts as part of a prospective study of neuropsychological, clinical, and imaging features associated with dementing illness in the elderly. All participants provided informed consent. The research was approved by our local research ethics committees.

Subjects

Between 1997 and 2000, 23 recruited 75 consecutive patients with ischemic vascular dementia (IVD, $n = 24$), Alzheimer's disease (AD, $n = 35$), or frontotemporal dementia (FTD, $n = 16$) from our cerebral function unit (a tertiary dementia referral unit), neurology department. All patients underwent detailed neurologic evaluation, neuropsychological assessment, MR imaging, and single photon emission CT with technetium-99m hexamethylpropyleneamine oxime at initial presentation.

IVD Group.—Patients with a clinical diagnosis of IVD fulfilled the National Institute of Neurological Disorders and Stroke–association Internationale pour la Recherche et l'Enseignement en Neurosciences criteria for possible IVD (33). Thirteen patients had a Hatchinski ischemic score of >7 (mean ± standard deviation [SD], 9.01 ± 1.66). The remaining 11 patients had a score of 3.96 ± 1.42. All patients had a clinical neurologic and neuropsychological deficit compatible with the clinical profile of IVD. None fulfilled the criteria for probable AD (34), the criteria for FTD (35, 36), or the criteria for Lewy body dementia (37). The diagnosis of IVD was carefully reevaluated every 6 months over a follow-up of 1–3 years. Equivocal cases were not included in the study.

AD Group.—All patients had neuropsychological deficits typical of AD, and all fulfilled the National Institute of Neurological and Communicative Diseases and Stroke–Alzheimer's Disease and Related Disorders Association criteria for probable AD (34). All patients who fulfilled clinical criteria for IVD, Lewy body disease (37), or FTD (35, 36) were excluded from this group regardless of whether or not they fulfilled criteria for AD.

FTD Group.—All patients fulfilled established criteria for FTD (35, 36), with a profound breakdown in personality and social conduct. On neuropsychological testing, these patients had significant frontal-lobe impairment with preserved visuospatial functions. All patients had a Hatchinski ischemic score of ≤3. Results of neurologic examination were normal or showed frontal-lobe release phenomena.

Control Subjects.—All control subjects came from the same four geographic areas. Some were spouses or partners of patients in the study, and some were recruited by means of advertisement.

Neuroimaging

Patients and control subjects were imaged by using a 1.5-T unit (ACS-NT, Power Track 6000 gradient subsystem; Philips Medical Systems, Best, the Netherlands) and a birdcage head coil receiver. The imaging protocol included the following axial sequences: 1) fluid-attenuated inversion recovery (FLAIR, TR/TE/TI = 11,000/140/2600, section thickness = 3.0 mm, no intersection gap), 2) T1-weighted inversion recovery (TR/TE/TI = 6850/18/300, section thickness = 3.0 mm), 3) variable-echo, fast spin echo (TR/TE1/TE2 = 5500/20/90, section thickness = 3.0 mm), and 4) high-resolution 3D T1-weighted fast field-echo (TR/TE = 24/18, section thickness = 0.89 mm, flip angle = 30°). For all sequences, the matrix was 256 × 256, and the FOV was 230 × 230 mm. Variable-echo and inversion recovery images were acquired with the same orientation and geometry as the FLAIR images. Inversion recovery images were reconstructed and viewed as real images in all cases.

Image Analysis

Deep WM and Periventricular Hyperintensities.—An experienced neuroradiologist (A.J.) blinded to the patient or subject group conducted all image analyses. Interobserver and Intraobserver variation the rating scale that we used was previously established in a group of 60 elderly patients with or without AD, FTD, IVD. The weighted Cohen κ values were 0.52–0.89 (good to excellent) for all components of the scale (32).

Images were transferred to a stand-alone personal computer workstation and viewed by using software (E Film Medical Ltd, Toronto, Ontario, Canada). Assessments was performed on matched T1-weighted inversion recovery and T2-weighted FLAIR images by using a scoring system based on the Schelten scale, which has four subscales (38). On the first subscales, frontal, parietal, and occipital periventricular hyperintensity was scored as follows: 0 for none, 1 for <5 mm thick, and 2 for >5 mm thick (total score of 0–6). On the other subscales, abnormalities in the deep WM hyperintensity (frontal, parietal, temporal, occipital), BG (lentiform and caudate nuclei, thalamus, internal capsule), and brainstem (cerebellar WM, midbrain and pontine reticular formations, medulla) were scored as follows: 0 for none; 1 for five or fewer ≤ 3 mm, 2 for six or more ≤ 3 mm, 3 for five or fewer 4–10 mm, 4 for six or more 4–10 mm, 5 for ≥11 mm, and 6 for confluent (total scores of 0–24).

Our scoring system differed from the original in that deep WM hyperintensity in the lentiform nucleus were treated as a single group and not split into lesions of the putaminal and globus pallidus. This change was made because of poor

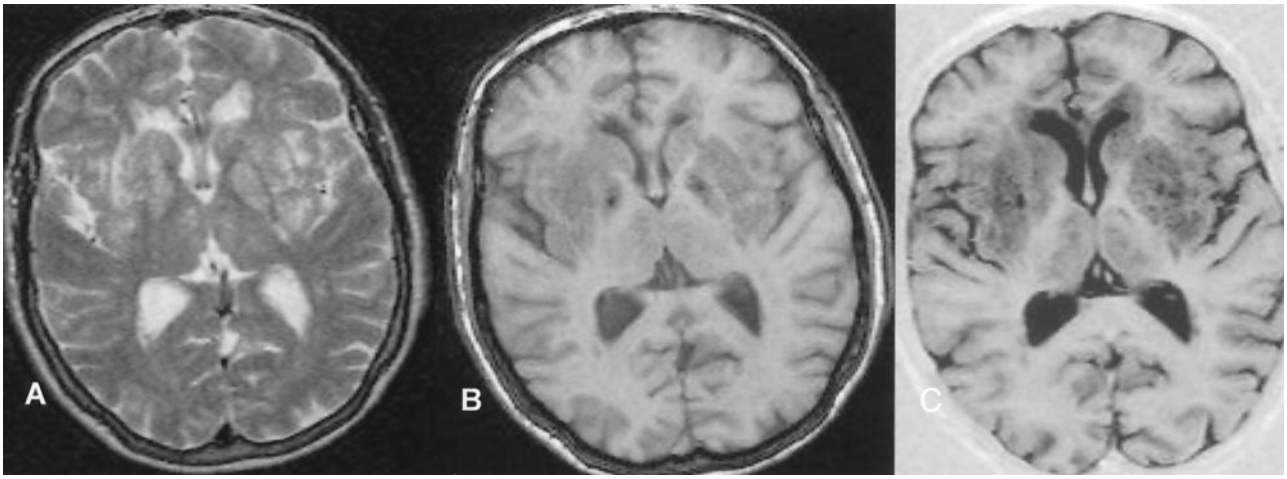

FIG 1. Matching axial MR images show severe (grade 5) dilatation of the VRS (matrix = 256 × 256, FOV = 230 × 230 mm): *A*, T2-weighted variable echo (TR/TE1/TE2 = 5500/20/90); *B*, T1-weighted high-spatial-resolution T1-weighted 3D gradient echo (TR/TE = 24/18, section thickness = 0.89 mm, flip angle = 30°); and *C*, inversion recovery (TR/TE/TE = 6850/18/300). Calculated CNRs for VRS versus WM are 64.1 for inversion recovery, 24.8 for fast field-echo, 19.1 for the variable-echo second-echo imaging.

TABLE 1: Adjusted Cohen κ scores for each component of the VRS scoring system

Component	Intraobserver 1	Intraobserver 2	Interobserver
BG			
Scheme 1	0.97	0.89	0.91
Scheme 2	1.0	0.96	0.98
Centrum semiovale	0.78	0.82	0.84
Subinsular	0.89	0.91	0.90
Mesencephalon	0.94	0.84	0.82

Note.—Intraobserver and interobserver variability assessed by using the Wilcoxon matched-pairs test.

repeatability of this aspect of the original scoring system in our practice.

Virchow-Robin Spaces.—Visualization of dilated VRSs was clearly improved by the use of heavily T1-weighted inversion recovery sequences compared with T2-weighted or high-resolution gradient-echo T1-weighted sequences. This improvement was confirmed by measuring contrast-to-noise ratios (CNRs) for enlarged VRSs for each sequence in a group of five subjects. CNR was calculated relative to WM as follows: $CNR = (S_{VRS} - S_{WM})/N$, where S_{VRS} is the mean signal intensity in the VRS, S_{WM} is the mean signal intensity in normal WM, and N is the background noise calculated as the width of the distribution of signal intensities in pure WM.

Calculated CNRs were 64.1 for inversion recovery, 24.8 for fast field-echo, 19.1 for variable-echo second-echo, and 1.9 for variable-echo first-echo imaging. On the basis of these findings, the VRS scores were based principally on the appearances seen on inversion recovery images (Fig 1). VRS were scored separately in the centrum semiovale (0 = none, 1 = less than five per side, 2 = more than five on one or both sides), the mesencephalon (0 = absent, 1 = present), and the subinsular region lateral to the lentiform nucleus (0 = none, 1 = less than five on either side, 2 = more than five on one or both sides). VRS in the BG were scored by using two scoring schemes (Table 1), the first of these (BG scheme 1) reflected the anatomic distribution of BG VRSs, and the second (BG scheme 2) reflected the distribution and number.

BG scheme 1 was as follows: 0 = VRS present only in the substantia innominata and fewer than five VRSs on either side, 1 = more than five VRS in the substantia innominata on either side or any VRS in the lentiform nucleus, and 2 = VRS in the caudate nucleus on either side. BG scheme 2 was as follows: 0 = VRS present only in the substantia innominata and fewer than five VRSs on either side, 1 = VRS only in the substantia innominata or more than five dilated VRS on either side, 2 = fewer than five in the lentiform nucleus on either side, 3 = five to 10 VRSs in the lentiform or fewer than five in the caudate nucleus on either side (Fig 2), 4 = more than 10 in the lentiform nucleus and fewer than five in the caudate nucleus on either side, 5 = more than 10 in lentiform nucleus and more than five in the caudate nucleus on either side (Fig 3).

When individual spaces were seen to extend through multiple images, these were counted as a single image (Fig 4). In cases of severe microvascular disease, the BG contains not only dilated VRS but also small cystic spaces, which may be due to lacunar infarction. It was not possible to confidently differentiate between dilated VRS and these small lacunae infarcts. In these cases, scores of 2 and 5 were allocated in BG schemes 1 and 2, respectively.

Two neuroradiologists (A.J., T.F.P.) who were blinded to the diagnosis independently performed the scoring. One week later, they repeated the scoring process in a subgroup of 50 patients to establish intraobserver reliability. The order of the subjects was randomized in both scoring sessions to eliminate training effects.

Cerebral Atrophy.—Cerebral atrophy was measured by using the technique Thacker et al described (39). The assessment was performed on inversion recovery images, and the technique provided an age- and head size–corrected index of prosencephalic atrophy beyond that expected with normal age-related loss. Age correction was not performed because the intention was to examine the relationship between atrophy and VRS dilatation.

Data and Statistical Analysis

Interobserver and intraobserver variability for the VRS scoring schemes was assessed by using the Wilcoxon matched pairs test to examine the hypothesis that the scores represent different populations, and a weighted Cohen κ test was used to quantify the level of agreement.

Statistical tests were performed to identify differences in scores between groups. We compared the control, AD, FTD, and IVD groups to test the hypothesis that indicators of microvascular disease are associated with subcortical vascular dementia. Differences between the ages of the subjects were compared by using analysis of variance with a posteriori Tukey test to allow us to identify between-group differences. All other variables were as-

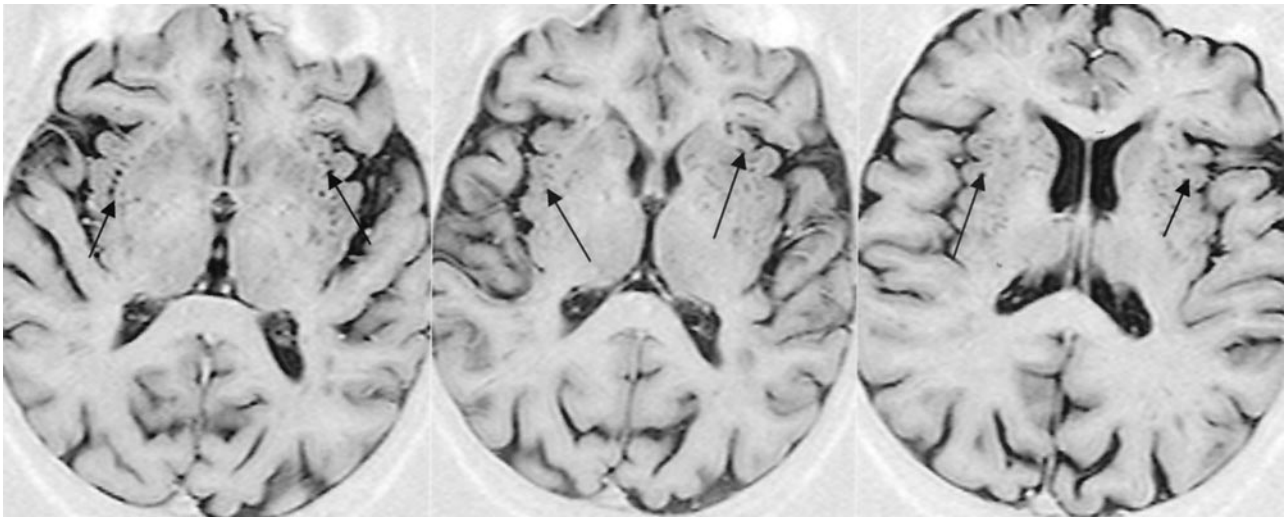

FIG 2. Axial inversion recovery MR images (TR/TE/TI = 6850/18/300, matrix = 256 × 256, FOV = 230 × 230 mm) show grade 3 VRS dilatation (*arrows*).

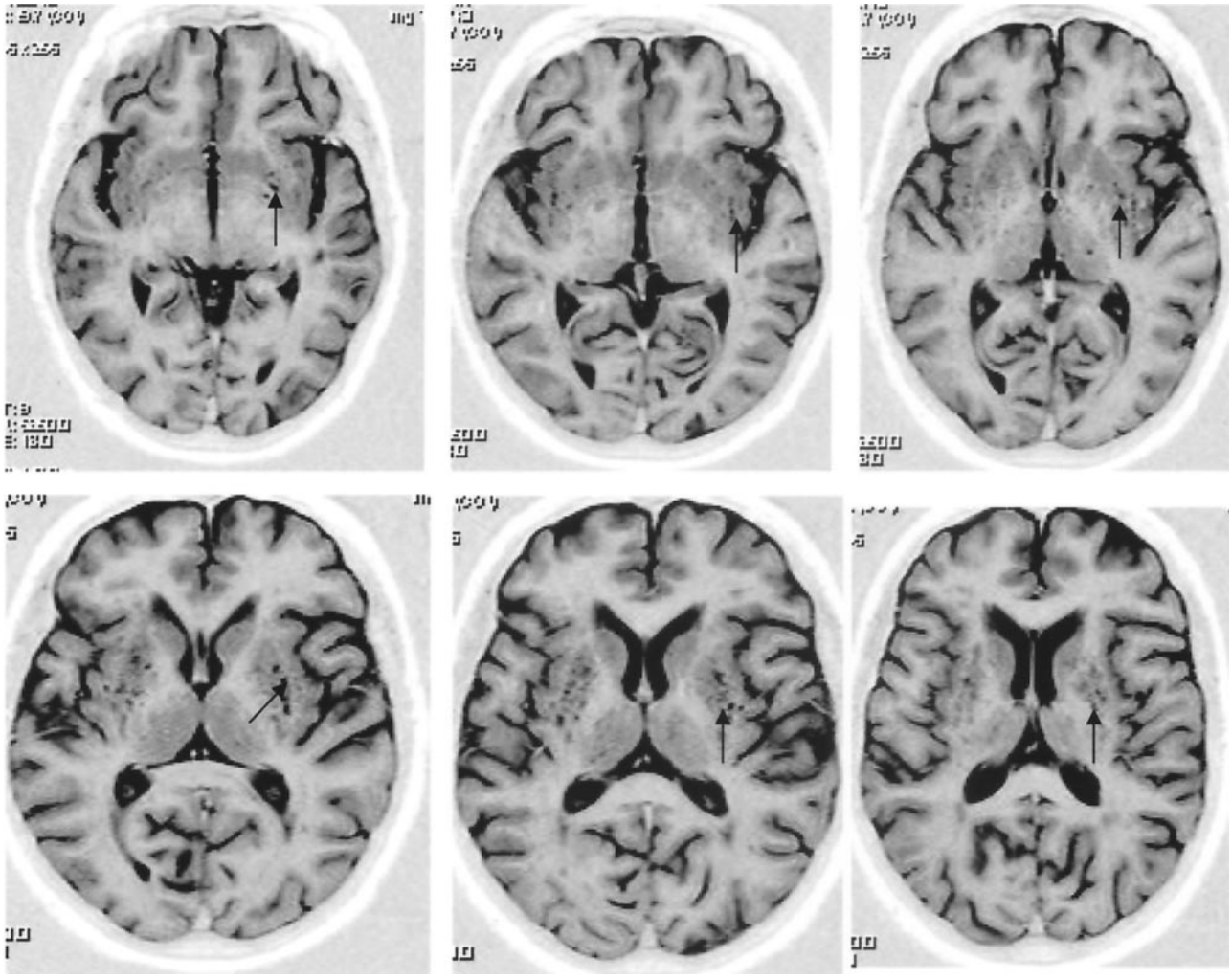

FIG 3. Axial inversion recovery MR images (TR/TE/TI = 6850/18/300, matrix = 256 × 256, FOV = 230 × 230 mm) show extensive VRS dilatation (*arrows*) throughout the BG (grade 5).

sessed by using the Kruskal-Wallis test with a posteriori Mann-Whitney *U* test to allow identification of between-group differences. Significance levels for the analysis of variance and Kruskal-Wallis test were set at $P < .05$. Significance levels for a posteriori tests were set at $P < .01$ to reduce the risks of type 1 errors.

Multiple regression analyses, with a forward stepwise

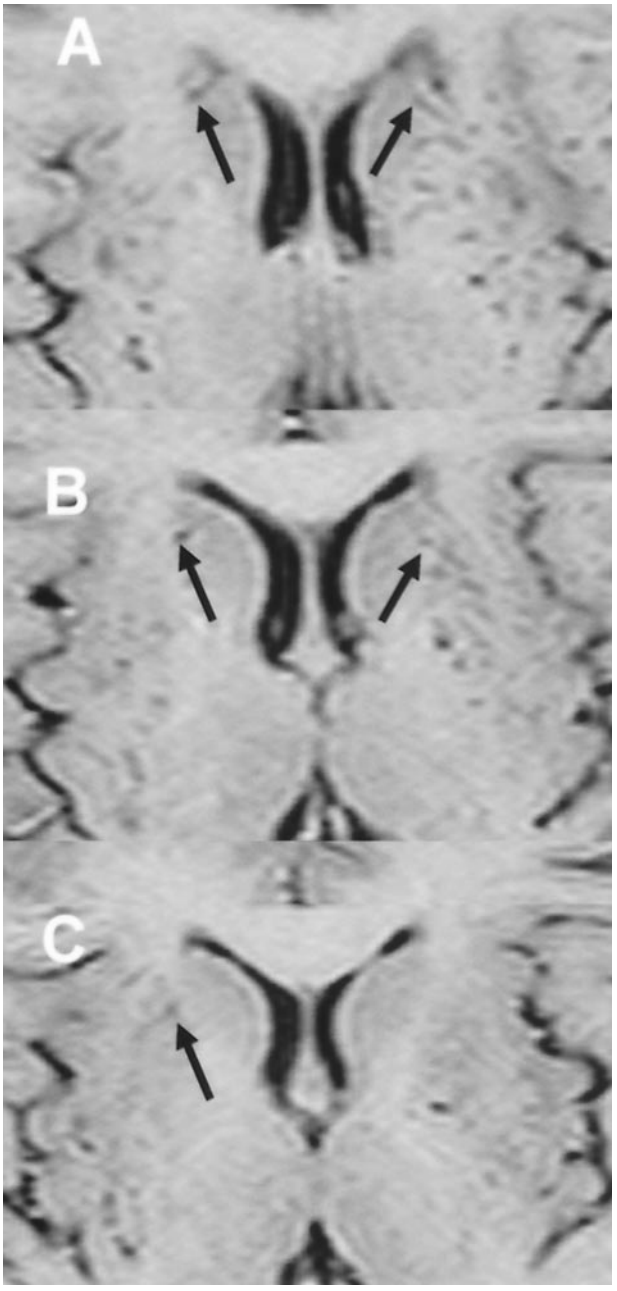

FIG 4. Axial Inversion recovery MR images (TR/TE/TI = 6850/18/300, matrix = 256 × 256, FOV = 230 × 230 mm) show the VRS (*arrows*) as linear structure passing through several sections (*A–C*) in the imaging volume.

method, were performed to identify the proportion of intergroup variance, which can be accounted for by individual variables. Variables included in the model were sex, age, diagnosis, periventricular hyperintensity score, BG hyperintensity score, deep WM hyperintensity score, VRS score from BG scheme 2, and VRS score in the centrum semiovale. The relationship between atrophy and diagnosis was tested by using an analysis of variance with a posteriori Tukey test to allow for the identification of between-group differences. The relationship between atrophy and VRS scores (BG scheme 2 and centrum semiovale) was tested by using regression analysis for each of the groups. The potential diagnostic sensitivity and specificity of the score from BG scheme 2 for IVD and of the score in the centrum semiovale for FTD were calculated at each of the available thresholds.

Results

VRS Scoring System

Interobserver and intraobserver variation in the VRS scoring systems was minimal, with no significant differences between scores. Cohen κ values demonstrated excellent agreement between scoring sessions for each observer (Table 1). Interobserver variation was also minimal, with no significant differences between observers and with excellent agreement on each component of the scoring systems. The lowest levels of agreement were seen for the scoring system applied to the centrum semiovale and the mesencephalon. Cohen κ scores for the BG and subinsular regions were high, reflecting failure of agreement in only one or two cases in the test dataset (Table 1).

Patients and Control Subjects

We enrolled 35 healthy volunteers (11 men, 24 women) aged 72.8 ± 6.56 years). Patients with dementia consisted of 35 patients with AD (18 men, 17 women) aged 61.6 ± 7.01 years, 16 patients (10 men, six women) with FTD aged 63.2 ± 9.24 years, and 24 patients (14 men, 10 women) with IVD aged 64.5 ± 7.35 years. Healthy volunteers were significantly older than the patients in the AD, FTD, and IVD groups ($P < .05$); this finding reflected the fact that younger individuals responded less frequently than older individuals to recruitment advertisements. Because VRS and WM lesions increase with age (2), age was included as a specific variable in the logistic regression analysis, although the older age of the healthy volunteers was expected to reduce the significance of any observed group differences in the comparisons of control and patient groups.

Table 2 shows the scores and statistical results for scores in WM lesions and VRSs. Significant group differences were seen in all components of the Scheltens score, with the exception of the infratentorial component. Each of these findings reflected a trend to higher scores in the IVD group. Significant group-to-group differences were observed on a posteriori tests; scores of periventricular hyperintensity, BG hyperintensity and overall scores were significantly greater in patients with IVD than in control subjects. Scores for the WM hyperintensities, periventricular hyperintensities, and total scores were significantly higher in patients with IVD than in those with AD.

Significant group differences were also seen in VRS scores in both the BG and the centrum semiovale (Table 2). Scores from BG schemes 1 and 2 were significantly higher in those with IVD than in patients with AD ($P < .001$), patients with FTD ($P < .01$), and healthy volunteers ($P < .005$ and $P < .001$, respectively). VRSs in the centrum semiovale were significantly more frequent in patients with FTD than in control subjects ($P < .01$).

Multiple regression analysis in patients with dementia showed that the VRS score from BG scheme 2 acted as an independent predictive factor, accounting for 29% of the variance in the regression model.

TABLE 2: WM-lesion and VRS scores

Result	Group					Control			AD		
	Control (n = 35)	AD (n = 35)	FTD (n = 24)	IVD (n = 16)	P Value	Vs AD	Vs FTD	Vs IVD	Vs FTD	Vs IVD	FTD vs IVD
Scheltens score											
Total	9.03 (7.31)	9.28 (5.24)	10.75 (8.02)	14.3 (10.1)	<.05	NS	NS	<.01	NS	<.01	NS
Deep WM total	5.14 (4.09)	5.26 (3.87)	5.65 (4.21)	9.26 (6.98)	<.05	NS	NS	NS	NS	<.01	NS
PVH	2.66 (1.94)	2.95 (2.16)	3.14 (3.02)	5.02 (4.26)	<.05	NS	NS	<.01	NS	<.01	NS
BG	0.77 (2.30)*	0.72 (1.89)	0.63 (1.28)	1.74 (2.15)	<.01	NS	NS	<.01	NS	NS	NS
Infratentorial	0.46 (0.74)	0.37 (0.64)	0.32 (0.30)	0.45 (0.61)	NS	NS	NS	NS	NS	NS	NS
BG											
Scheme 1	0.86 (0.88)	0.82 (0.88)	1.06 (0.80)	1.92 (0.83)	<.005	NS	NS	<.005	NS	<.001	NS
Scheme 2	1.46 (1.20)	1.29 (1.26)	2.0 (1.12)	3.92 (0.99)	<.001	NS	NS	<.001	NS	<.001	<.01
Centrum semiovale	0.51 (0.85)	0.74 (0.60)	1.33 (0.70)	1.03 (0.39)	<.01	NS	<0.01	<.01	NS	NS	NS
Subinsular	0.96 (1.95)	0.47 (0.51)	0.67 (0.72)	1.17 (0.39)	NS	NS	NS	NS	NS	NS	NS
Mesencephalic	0.51 (0.51)	0.65 (0.49)	0.73 (0.46)	0.92 (0.28)	NS	NS	NS	NS	NS	NS	NS

Note.—Differences in ages were compared by using ANOVA (at $P < .05$) with an a posteriori Tukey test (at $P < .01$). Other variables were assessed by using the Kruskal-Wallis test (at $P < .05$) with an a posteriori Mann-Whitney U test (at $P < .01$) to identify between-group differences. NS = not significant. Data in parentheses are total number of patients in each group. The score is the SD of the measurement.

TABLE 3: Sensitivities and specificities based on BG2 cutoff values as indicators of vascular dementia

Comparison	BG2 VRS Score		
	>2	>3	>4
IVD vs AD and FTD			
Sensitivity	0.67	0.54	0.25
Specificity	0.70	0.87	1
IVD vs AD			
Sensitivity	0.67	0.54	0.25
Specificity	0.89	0.93	1
IVD vs FTD			
Sensitivity	0.67	0.54	0.25
Specificity	0.76	0.93	1

TABLE 4: Sensitivities and specificities based on centrum-semiovale cutoff values as indicators of vascular dementia

Comparison	Centrum Semiovale VRS Score	
	>0	>1
FTD vs AD and IVD		
Sensitivity	0.81	0.38
Specificity	0.27	0.25
FTD vs AD		
Sensitivity	0.81	0.38
Specificity	0.39	0.50
FTD vs IVD		
Sensitivity	0.81	0.38
Specificity	0.45	0.33

The VRS score in the centrum semiovale accounted for a further 9%, and the Scheltens score for periventricular hyperintensity accounted for another 2%.

Table 3 shows the sensitivity and specificity values that would have been obtained in the current dataset if the BG scheme 2 VRS score had been used as a diagnostic marker, and it shows the effect of selecting different cutoff values on the identification of IVD from FTD and AD. Table 4 shows the sensitivity and specificity values that would have been obtained if the centrum semiovale VRS score had been used to differentiate patients with FTD from those with AD and IVD.

Cerebral Atrophy

Measures of cerebral atrophy corrected for head size significantly differed between groups ($P < .001$). Pairwise comparison showed greater atrophy in the FTD and AD groups compared with control subjects ($P < .0001$ and $P < .001$, respectively); these findings are in keeping with those of previous studies (39). BG-VRS2 score was not significantly correlated atrophy in any of the groups. VRS score in the centrum semiovale was significantly and positively correlated with atrophy in patients with FTD ($R^2 = 0.43$, $P < .01$) and in those with IVD ($R^2 = 0.24$, $P < .05$).

Discussion

VRSs are potential perivascular spaces covered by pia that accompany arteries and arterioles as they perforate the brain substance. Deep in the brain, the VRS are lined by the basement membrane of the glia limitans peripherally, while the outer surfaces of the blood vessels lie centrally. These pial layers form the VRS as enclosed spaces filled with interstitial fluid and separated from the surrounding brain and CSF (6, 40). Dilatation of VRS results in fluid filled perivascular spaces along the course of the penetrating arteries.

Abnormal dilatation of VRS is clinically associated with aging, dementia, incidental WM lesions, and hypertension and other vascular risk factors (2, 5). Pathologically, this finding is most commonly associated with arteriosclerotic microvascular disease, which forms a spectrum of severity graded from 1 to 3 on the basis of histologic appearances (22, 24). Grade 1 changes include increased tortuosity and irregularity in small arteries and arterioles (22) Grade

2 changes include progress sclerosis, hyalinosis, lipid deposits, and regional loss of smooth muscle in the vessel wall associated with lacunar spaces that are histologically seen to consist of three subtypes. Type 1 lacunes are small, old cystic infarcts; type 2 are scars of old hematomas; and type 3 are dilated VRS (41). Grade 3 microangiopathy represents the most severe stage and is especially related to severe chronic hypertension. Typical changes described in lower grades are accompanied by fibrotic thickening vessel wall with onion skinning, loss of muscularis and elastic lamina, and regional necrosis in the vessel walls. The brain parenchyma contains multiple lacunae, and diffuse abnormality of myelin is present in the deep hemispheric WM.

Several mechanisms for abnormal dilatation of VRS have been suggested (42, 43). These include mechanical trauma due to CSF pulsation or vascular ectasia (2, 44), fluid exudation due to abnormalities of the vessel wall permeability (45, 46), and ischemic injury to perivascular tissue causing a secondary ex vacuo effect (47).

In the Western world, IVD is seen in 8–10% of cognitively impaired elderly subjects (48) and commonly associated with widespread small ischemic or vascular lesions throughout the brain, with predominant involvement of the BG, WM, and hippocampus (48). Several groups have shown that a severe lacunar state and microinfarction due to arteriolosclerosis and hypertensive microangiopathy are more common in individuals with IVD than in healthy control subjects, and they have emphasized the importance of small vascular lesions in the development of dementia (19, 21, 48, 49).On CT or MR imaging, WM lesions are commonly used as potential biomarkers of vascular abnormality. Many groups have suggested that simple scoring schemes for WM lesion load and distribution are useful in the diagnosis of vascular dementia (50–53). Although WM lesions are more severe in patients with vascular dementia (32, 50, 54–57), they are more prevalent in all groups with dementia than in healthy control subjects.

Dilation of VRS provides a potential alternative biomarker of microvascular disease. To our knowledge, the relationship between dilated VRS identified on MR imaging and the diagnostic classification and other imaging features of dementing illnesses have not be studies. Our results show that a VRS score on BG scheme 2 of >2 achieves a sensitivity of 67% and specificity of 70% in differentiating IVD from AD or FTD, whereas a score of >4 decreases the sensitivity to 25% but improve the specificity to 100%. Multiple regression analysis in patients with dementia showed that the score on BG scheme 2 acted as an independent predictor accounting for 29% of the variance in the regression model, but the Scheltens PVH score accounted for only an additional 2%. VRS BG scheme 2 is simple, quick to perform, and highly reproducible.

VRSs in the centrum semiovale were significantly more frequent in patients with FTD than in control subjects ($P < .01$). This finding is not associated with increases in BG VRS and is closely correlated with measures of forebrain atrophy, suggesting that these changes are probably representative of atrophy, which is more marked in this patient group than in those with other dementing conditions (39).

We believe that the findings outlined here have considerable potential importance in the investigation of brain diseases in the aging population. However, our study had clear limitations. We believe our study represents the first of its type, and the samples were relatively small. We deliberately selected patients with early-onset dementia who are consequently young compared with a population with mixed dementias. This approach reflects clinical practice in which new therapeutic measures are primarily targeted at young patients with clear clinical syndromes who have less evidence of mixed etiologic contributions. Of note, our control population was significantly older than those with dementia. This difference reflected local recruitment problems but is a potential source of bias in the study. However, in practice, one would anticipate that an older healthy population has an increased incidence of microangiopathic changes, which would be expected to decrease the significance of the findings described here. Furthermore, aging did not appear as an independent significant correlate of VRS dilatation in the multiple regression analysis. Another potential criticism is related to the identification of dilated VRS. In most cases in which the number of lesions is relatively small, it is possible to be confident that this finding represents VRS because their linear structure can be seen passing through several sections in the imaging volume (Fig 4). In more severe cases (grade 5 in BG scheme 2), the lesions were often so numerous that this structural feature could not be identified with confidence. Results of previous histologic studies suggest that, in many of these cases, the lesions scored represent an admixture of dilated VRS and small (type 1) lacunes. We have taken a pragmatic approach to this, including all of the lesions in the scoring system because existing pathologic evidence suggests that these lesions share common etiologic mechanisms.

Conclusion

Semiquantitative estimation of the number and distribution of dilated VRS appears to hold promise as a surrogate marker of cerebral microvascular disease. Previous pathologic studies have shown that VRS dilatation is common in diseases associated with microvascular abnormality, and our findings suggest that MR imaging evidence of VRS dilatation may aid in the differentiation of vascular dementias from degenerative dementias. We provide a simple, subjective scoring system that is adequate, quick to apply, and highly reproducible. The diagnostic sensitivities and specificities are sufficient to suggest clinical value in their use, although a combination with other indicators (e.g., measurements of atrophy) may be confidently expected to provide further improvement. The

pattern of distribution (i.e., vertex vs. BG) may represent different etiologies of VRS dilatation and provide additional information in individual cases.

References

1. Hirabuki N, Fujita N, Fujii K, Hashimoto T, Kozuka T. **MR appearance of Virchow-Robin spaces along lenticulostriate arteries: spin-echo and two-dimensional fast low-angle shot imaging.** *AJNR Am J Neuroradiol* 1994;15:277–281
2. Heier LA, Bauer CJ, Schwartz L, Zimmerman RD, Morgello S, Deck MD. **Large Virchow-Robin spaces: MR-clinical correlation.** *AJNR Am J Neuroradiol* 1989;10:929–936
3. Braffman BH, Zimmerman RA, Trojanowski JQ, Gonatas NK, Hickey WF, Schlaepfer WW. **Brain MR: pathologic correlation with gross and histopathology. 1. Lacunar infarction and Virchow-Robin spaces.** *AJR Am J Roentgenol* 1988;151:551–558
4. Machado MA Jr, Matos AS, Goyanna F, Barbosa VA, Vieira LC. **[Dilatation of Virchow-Robin spaces in patients with migraine].** *Ar Qneuropsiquiatr* 2001;59:206–209
5. Bokura H, Kobayashi S, Yamaguchi S. **Distinguishing silent lacunar infarction from enlarged Virchow-Robin spaces: a magnetic resonance imaging and pathological study.** *J Neurol* 1998;245:116–122
6. Ozturk MH, Aydingoz U. **Comparison of MR signal intensities of cerebral perivascular (Virchow-Robin) and subarachnoid spaces.** *J Comput Assist Tomogr* 2002;26:902–904
7. Achiron A, Faibel M. **Sandlike appearance of Virchow-Robin spaces in early multiple sclerosis: a novel neuroradiologic marker.** *AJNR Am J Neuroradiol* 2002;23:376–380
8. Afifi AK. **Enlarged Virchow-Robin spaces along the medullary perforators in a child with seizures.** *J Neuroimaging* 1996;6:197–198
9. Di Costanzo A, Di Salle F, Santoro L, Bonavita V, Tedeschi G. **Dilated Virchow-Robin spaces in myotonic dystrophy: frequency, extent and significance.** *Eur Neurol* 2001;46:131–139
10. Schick S, Gahleitner A, Wober-Bingol C, et al. **Virchow-Robin spaces in childhood migraine.** *Neuroradiology* 1999;41:283–287
11. Simpson SW, Jackson A, Baldwin RC, Burns A. **1997 IPA/Bayer Research Awards in Psychogeriatrics: subcortical hyperintensities in late-life depression: acute response to treatment and neuropsychological impairment.** *Int Psychogeriatr* 1997;9:257–275
12. Andreula CF, Burdi N, Carella A. **CNS cryptococcosis in AIDS: spectrum of MR findings.** *J Comput Assist Tomogr* 1993;17:438–441
13. Artigas J, Poo P, Rovira A, Cardo E. **Macrocephaly and dilated Virchow-Robin spaces in childhood.** *Pediatr Radiol* 1999;29:188–190
14. Auer RN, Budny J, Drake CG, Ball MJ. **Frontal lobe perivascular schwannoma. Case report.** *J Neurosurg* 1982;56:154–157
15. Bastos AC, Andermann F, Melancon D, et al. **Late-onset temporal lobe epilepsy and dilatation of the hippocampal sulcus by an enlarged Virchow-Robin space.** *Neurology* 1998;50:784–787
16. Campi A, Benndorf G, Filippi M, Reganati P, Martinelli V, Terreni MR. **Primary angiitis of the central nervous system: serial MRI of brain and spinal cord.** *Neuroradiology* 2001;43:599–607
17. Castaldo JE, Bernat JL, Meier FA, Schned AR. **Intracranial metastases due to prostatic carcinoma.** *Cancer* 1983;52:1739–1747
18. Chuang YC, Lui CC, Hsu SP, Chang CS, Lin TK. **Unusual dilatation of Virchow-Robin spaces: case report.** *Changgeng Yi Xue Za Zhi* 1999;22:671–675
19. Esiri MM WG, Morris JH. **Neuropathological assessment ofthe lesions of significance in vascular dementia.** *J Neurol Neurosurg Psychiatry* 1997;63:749–753
20. Rollins NK, Deline C, Morriss MC. **Prevalence and clinical significance of dilated Virchow-Robin spaces in childhood.** *Radiology* 1993;189:53–57
21. Erkinjuntti T, Benavente O, Eliasziw M, et al. **Diffuse vacuolization (spongiosis) and arteriolosclerosis in the frontal white matter occurs in vascular dementia.** *Arch Neurol* 1996;53:325–332
22. Hommel M, Gray F. **Microvascular pathology.** In: Caplan L, ed. *Brain Ischaemia: Basic Concepts and Clinical Relevance.* New York: Springer-Verlag *Berlin*; 1995:215–223
23. Furuta A, Ishii N, Nishihara Y, Horie A. **Medullary arteries in aging and dementia.** *Stroke* 1991;22:442–446
24. Brun A, Fredriksson K, Gustafson L. **Pure subcortical arteriosclerotic encephalopathy (Binswanger's disease): a clinicopathological study. Part 2: Pathological features.** *Cerebrovasc Dis* 1992;2:87–92
25. Thomas AJ, O'Brien JT, Davis S, et al. **Ischemic basis for deep white matter hyperintensities in major depression: a neuropathological study.** *Arch Gen Psychiatry* 2002;59:785–792
26. Thomas AJ, Perry R, Barber R, Kalaria RN, O'Brien JT. **Pathologies and pathological mechanisms for white matter hyperintensities in depression.** *Ann N Y Acad Sci* 2002;977:333–339
27. Thomas AJ, Perry R, Kalaria RN, Oakley A, McMeekin W, O'Brien JT. **Neuropathological evidence for ischemia in the white matter of the dorsolateral prefrontal cortex in late-life depression.** *Int J Geriatr Psychiatry* 2003;18:7–13
28. Krishnan KR, McDonald WM. **Arteriosclerotic depression.** *Med Hypotheses* 1995;44:111–115
29. Krishnan KR, Hays JC, Blazer DG. **MRI-defined vascular depression.** *Am J Psychiatry* 1997;154:497–501
30. Alexopoulos GS, Meyers BS, Young RC, Campbell S, Silbersweig D, Charlson M. **"Vascular depression" hypothesis.** *Arch Gen Psychiatry* 1997;54:915–922
31. Greenwald BS, Kramer-Ginsberg E, Krishnan KR, et al. **A controlled study of MRI signal hyperintensities in older depressed patients with and without hypertension.** *J Am Geriatr Soc* 2001;49:1218–1225
32. Varma AR, Laitt R, Lloyd JJ, et al. **Diagnostic value of high signal abnormalities on T2 weighted MRI in the differentiation of Alzheimer's, frontotemporal and vascular dementias.** *Acta Neurol Scand* 2002;105:355–364
33. Roman GC, Tatemichi TK, Erkinjuntti T, et al. **Vascular dementia: diagnostic criteria for research studies: report of the NINDS-AIREN International Workshop.** *Neurology* 1993;43:250–260
34. McKhann G, Drachman D, Folstein M, Katzman R, Price D, Stadlan EM. **Clinical diagnosis of Alzheimer's disease: report of the NINCDS-ADRDA Work Group under the auspices of Department of Health and Human Services Task Force on Alzheimer's Disease.** *Neurology* 1984;34:939–944
35. Brun A, Gustafson L, Passant U. **A new kind of degenerative dementia: localization, rather than type is significant in frontal lobe dementia.** *Lakartidningen* 1994;91:4751–4757
36. Neary D, Snowden JS, Gustafson L, et al. **Frontotemporal lobar degeneration: a consensus on clinical diagnostic criteria.** *Neurology* 1998;51:1546–1554
37. McKeith IG, Perry RH, Fairbairn AF, Jabeen S, Perry EK. **Operational criteria for senile dementia of Lewy body type (SDLT).** *Psychol Med* 1992;22:911–922
38. Scheltens P, Barkhof F, Leys D, et al. **A semiquantative rating scale for the assessment of signal hyperintensities on magnetic resonance imaging.** *J Neurol Sci* 1993;114:7–12
39. Thacker NA, Varma AR, Bathgate D, et al. **Dementing disorders: volumetric measurement of cerebrospinal fluid to distinguish normal from pathologic findings: feasibility study.** *Radiology* 2002;224:278–285
40. Zhang ET, Inman CB, Weller RO. **Interrelationships of the pia mater and the perivascular (Virchow-Robin) spaces in the human cerebrum.** *J Anat* 1990;170:111–123
41. Poirier J, Derouesne C. **Cerebral lacunae: a proposed new classification [letter].** *Clin Neuropathol* 1984;3:266
42. Fazekas F, Kleinert R, Offenbacher H, et al. **The morphologic correlate of incidental punctate white matter hyperintensities on MR images.** *AJNR Am J Neuroradiol* 1991;12:915–921
43. Ogawa T, Okudera T, Fukasawa H, et al. **Unusual widening of Virchow-Robin spaces: MR appearance.** *AJNR Am J Neuroradiol* 1995;16:1238–1242
44. Hughes W. **Origin of lacunes.** *Lancet* 1965 1:19–21
45. Benhaiem-Sigaux N, Gray F, Gherardi R, Roucayrol AM, Poirier J. **Expanding cerebellar lacunes due to dilatation of the perivascular space associated with Binswanger's subcortical arteriosclerotic encephalopathy.** *Stroke* 1987;18:1087–1092
46. Derouesne C, Gray F, Escourolle R, Castaigne P. "**Expanding cerebral lacunae" in a hypertensive patient with normal pressure hydrocephalus.** *Neuropathol Appl Neurobiol* 1987;13:309–320
47. Pullicino PM, Miller LL, Alexandrov AV, Ostrow PT. **Infraputaminal "lacunes": clinical and pathological correlations.** *Stroke* 1995;26:1598–1602
48. Jellinger KA. **The pathology of ischemic-vascular dementia: an update.** *J Neurol Sci* 2002; 203–204:153–157
49. Hulette C ND, McKeel D, Morris K, Mirras SS, Sumi SM, et. a. **Clinical-neuropathologic findings in multi-infarct dementia: a reportof six autopsied cases**. *Neurology* 1997;48:668–672
50. Erkinjuntti T. **Diagnosis and management of vascular cognitive impairment and dementia**. *J Neural Transm* Suppl 2002:91–109
51. Hentschel F, Kreis M, Damian M, Krumm B. **Microangiopathic**

lesions of white matter: quantitation of cerebral MRI findings and correlation with psychological tests. *Nervenarzt* 2003;74:355–361
52. Wahlund LO, Basun H, Almkvist O, Andersson-Lundman G, Julin P, Saaf J. **White matter hyperintensities in dementia: does it matter?** *Magn Reson Imaging* 1994;12:387–394
53. Leys D, Pasquier F, Lucas C, Pruvo JP. **Magnetic resonance imaging in vascular dementia.** *J Mal Vasc* 1995;20:194–202
54. Barber R, Scheltens P, Gholkar A, et al. **White matter lesions on magnetic resonance imaging in dementia with Lewy bodies, Alzheimer's disease, vascular dementia, and normal aging.** *J Neurol Neurosurg Psychiatry* 1999;67:66–72
55. Chui H. **Dementia due to subcortical ischemic vascular disease.** *Clin Cornerstone* 2001;3:40–51
56. Pasquier F, Henon H, Leys D. **Relevance of white matter changes to pre- and poststroke dementia.** *Ann N Y Acad Sci* 2000;903:466–469
57. Udaka F, Sawada H, Kameyama M. **White matter lesions and dementia: MRI-pathological correlation.** *Ann N Y Acad Sci* 2002; 977:411–415